








RESEARCH ARTICLE | JUNE 12 2023

Nonspecific eddy current heating in magnetic field hyperthermia

Martin K. Y. Kwok ; Cliona C. J. Maley ; Asher Dworkin ; Simon Hattersley ; Paul Southern ; Quentin A. Pankhurst  



Appl. Phys. Lett. 122, 240502 (2023)

<https://doi.org/10.1063/5.0153336>



View
Online



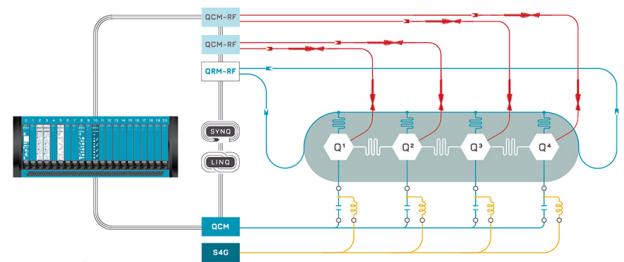
Export
Citation

CrossMark



Integrates all
Instrumentation + Software
for Control and Readout of

Superconducting Qubits
NV-Centers
Spin Qubits



Superconducting Qubit Setup

[find out more >](#)

Nonspecific eddy current heating in magnetic field hyperthermia

Cite as: Appl. Phys. Lett. **122**, 240502 (2023); doi: [10.1063/5.0153336](https://doi.org/10.1063/5.0153336)

Submitted: 6 April 2023 · Accepted: 24 May 2023 ·

Published Online: 12 June 2023



View Online



Export Citation



CrossMark

Martin K. Y. Kwok,¹  Cliona C. J. Maley,¹  Asher Dworkin,¹  Simon Hattersley,²  Paul Southern,² 
and Quentin A. Pankhurst^{1,2,a)} 

AFFILIATIONS

¹UCL Healthcare Biomagnetics Laboratory, University College London, 21 Albemarle Street, London W1S 4BS, United Kingdom

²Resonant Circuits Limited, 21 Albemarle Street, London W1S 4BS, United Kingdom

^{a)} Author to whom correspondence should be addressed: q.pankhurst@ucl.ac.uk

ABSTRACT

In this Perspective article, we explore the definition and use of clinical tolerability metrics associated with nonspecific eddy current heating in magnetic field hyperthermia (MFH). We revisit the origins of the “Brezovich criterion,” $H_o f \leq 485 \text{ MA m}^{-1} \text{ s}^{-1}$, as it is applied to axial time-varying magnetic fields $H(t) = H_o \sin(2\pi ft)$ and the human torso. We then consider alternative metrics, including the “maximal specific absorption rate” (SAR_{max}) of eddy-current-induced power absorbed per unit mass of tissue. With reference to previously published clinical data and the results of two volunteer studies in our laboratory, we show that the SAR_{max} metric is both suitable and reliable. We also show how it may be extracted from *in silico* finite element models to cope with confounding effects such as anatomical hot spots and non-axial-field geometries. We note a parallel with a standardized metric, the “local SAR” used in magnetic resonance imaging (MRI). We suggest that the limits established in clinical MRI (that the local SAR, averaged over 10 g of tissue and 6 min of treatment, should not exceed 20 mW g^{-1} in the torso or head, and 40 mW g^{-1} in the limbs) might be regarded as a good starting point for the design of MFH interventions. We conclude with the recommendation that the SAR_{max} metric is adopted for future use in the development of clinically safe and tolerable MFH equipment.

© 2023 Author(s). All article content, except where otherwise noted, is licensed under a Creative Commons Attribution (CC BY) license (<http://creativecommons.org/licenses/by/4.0/>). <https://doi.org/10.1063/5.0153336>

I. INTRODUCTION

In magnetic field hyperthermia (MFH), a time-varying magnetic field $H(t) = H_o \sin(2\pi ft)$ is used to deliver thermal energy into implanted magnetic materials in the human body, for therapeutic purposes.¹ The implanted materials are typically injectable magnetic nanoparticle suspensions,^{2,3} albeit there is also interest in millimeter-scale thermal seeds.⁴ Currently, MFH is used clinically in the treatment of glioblastoma and prostate cancer⁵ and is being tested for pancreatic cancer.⁶ It is also the subject of extensive *in vitro* and preclinical testing as researchers explore ways to optimize and use it.⁷

Although the focus of MFH is on heating the implanted materials, all mammalian tissues are electrically conductive due to their high water content, and as such, the time-varying magnetic fields induce circulating electrical currents (eddy currents) in accordance with Faraday’s law of induction. This “nonspecific” tissue heating—meaning that part of the tissue heating which is not associated with the implanted materials and, as such, does not necessarily affect the intended treatment region—appears alongside, and in addition to,

the intended MFH heating of the implanted materials. As such, it is a potentially treatment-limiting source of thermal loading that may be delivered to the patient during MFH.

Both clinically and theoretically, eddy current heating was considered in some detail in the early 1980s in relation to an early variant of MFH that utilized a single-turn magnetic field generator known as a “Magnetode.”^{8–12} Shortly thereafter, Brezovich and co-workers reported on a human tolerance study, from which they concluded that a useful rule-of-thumb for whole-body MFH systems was that to avoid excessive nonspecific eddy current heating, the product $H_o f$ should not exceed $485 \text{ MA m}^{-1} \text{ s}^{-1}$.^{13,14} Subsequently, the Brezovich criterion has been widely used in the evaluation of prospective clinical applications of MFH,¹⁵ while, at the same time, it has become the subject of much discussion, as researchers have debated both its merits and its applicability.^{16–24}

In this Perspective article, we explore the definition and use of tolerability metrics in MFH. We begin by revisiting the theoretical origins of the Brezovich criterion, recalling the experimental conditions to which it applies and reminding ourselves how to apply it to different

geometries and tissue types. We then consider other metrics, including the “maximal specific (per unit mass of tissue) absorption rate” SAR_{\max} , which we believe may be preferable for safety and design purposes. We apply the SAR_{\max} approach to data collected in two human volunteer studies in which MFH-style time-varying magnetic fields were applied to participants’ arms, legs, and torsos. These data include tests using a new clinical MFH system.⁶ We further investigate the SAR_{\max} method through comparisons with finite element analysis models of relevance to the volunteer studies. Finally, we review and consider prospects for future research and development in this field.

II. THEORY

Oleson¹¹ provides a succinct derivation of the analytic formulas governing power deposition into a cylindrically symmetric load aligned coaxially with a cylindrically symmetric applied magnetic field, summarized as follows.

We define a coordinate system $(\hat{r}, \hat{\theta}, \hat{z})$ in which the time-varying applied field \mathbf{H} is aligned along $(0, 0, \hat{z})$,

$$\mathbf{H} = H \hat{z} = H_0(r) e^{i\omega t} \hat{z}, \quad (1)$$

where $\omega = 2\pi f$ is the angular frequency and where we assume that the field is axially symmetric but may vary radially. Faraday’s law in the integral form is

$$\oint \mathbf{E} \cdot d\mathbf{l} = - \frac{\partial}{\partial t} \int \mu_0 \mathbf{H} \cdot \mathbf{n} dS, \quad (2)$$

where \mathbf{E} is the induced electric field, $d\mathbf{l}$ is a line element along a closed contour, and \mathbf{n} is a unit vector normal to the surface element dS . [N.B.: Strictly speaking, the permeability μ of the load medium should be used in Eq. (2) rather than μ_0 , but, given that in biological tissues, μ is very close to the permeability of free space—e.g., $\mu_{\text{water}} = 0.999992 \mu_0$ —the difference is negligible.]

Given the assumed symmetry of \mathbf{H} , it follows that the induced \mathbf{E} field will be tangential [i.e., $\mathbf{E} = E(r) \hat{\theta}$], so that

$$\oint \mathbf{E}(r) \cdot d\mathbf{l} = 2\pi r E(r) = -i\omega \mu_0 \int_0^r H_0(r') 2\pi r' dr', \quad (3)$$

$$\therefore E(r) = - \frac{i\omega \mu_0}{r} \int_0^r H_0(r') r' dr'. \quad (4)$$

The power density, in W m^{-3} (or sometimes reported in mW cm^{-3} for convenient reference to tissue loading), associated with this field is

$$P_v(r) = \frac{1}{2} \sigma E E^*, \quad (5)$$

where E^* is the complex conjugate of E and σ is the electrical conductivity of the load, in S m^{-1} . The general solution for Eq. (5), using Eq. (4), is then

$$P_v(r) = \frac{\sigma \omega^2 \mu_0^2}{2r^2} \left[\int_0^r H_0(r') r' dr' \right]^2. \quad (6)$$

In the special case, where the magnetic field is uniform throughout the volume of the load, so that $H_0(r') = H_0$ for all r' in the range from 0 to r , this reduces to the form

$$P_v(r) = \frac{1}{8} \sigma \omega^2 \mu_0^2 H_0^2 r^2 \quad (7)$$

$$= \frac{1}{2} \sigma \pi^2 \mu_0^2 H_0^2 f^2 r^2. \quad (8)$$

Finally, if the magnetic field extends over a cylindrical load volume of length L and radius R , the total power deposited into that volume is

$$P_{\text{total}} = L \int_0^R P_v(r) 2\pi r dr = \frac{1}{16} L \pi \sigma \omega^2 \mu_0^2 H_0^2 R^4. \quad (9)$$

Equations (7)–(9) are frequently cited in the literature and were used to derive the Brezovich criterion. [N.B.: Note that there is a typographical error in Atkinson *et al.*,¹³ where the pre-factor $\frac{1}{2}$ in Eq. (8) is missing.]

It may be noted that the derivation earlier assumes that there is negligible attenuation of the applied magnetic fields due to the induced eddy currents. This assumption has been tested *in silico* for cylinders of muscle-equivalent tissue of radius up to the 15 cm of a typical human torso.²⁵ As expected for electromagnetic field effects, the attenuation is frequency dependent: for f up to 1 MHz, it is $\leq 1\%$; at 5 MHz, $\leq 2\%$; and at 13.56 MHz, $\leq 8\%$. Given that contemporary MFH generally operates in the range 100 to 350 kHz, the assumption of negligible attenuation looks to be a valid approximation in practice.

III. COMMENTARY ON THE BREZOVICH CRITERION AND OTHER TOLERABILITY METRICS

The Brezovich criterion, $H_0 f \leq 485 \text{ MA m}^{-1} \text{ s}^{-1}$, was experimentally determined to be a physiologically tolerable level of prolonged exposure (more than 1 h) to the torso.^{13,14} Volunteers lying on a gurney bed were axially positioned within a 30 cm wide single-turn coil operating at $f = 13.56 \text{ MHz}$, and the current was increased until the power loading (the amount of power dissipated in the tissue) was 200 W—a value that the authors selected based on modeling and on “the extensive clinical experience with the Magnetronde.”¹⁴ In one particular individual, the field amplitude at the 200 W loading was found to be 36.2 A m^{-1} , giving $H_0 f = 491 \text{ MA m}^{-1} \text{ s}^{-1}$. The criterion value was set to be a little lower than this, at $H_0 f = 485 \text{ MA m}^{-1} \text{ s}^{-1}$.

From this description, it is clear that a key step in the derivation of the Brezovich criterion limit was the assumption that 200 W was an acceptable power loading to the adult torso, with the key justification for this resting on clinical experience with the Magnetronde. At that time (the early 1980s), the Magnetronde had already been used clinically for many years, with published reports including data from more than 3000 treatments.¹² The Magnetronde had a very simple design, comprising a single rolled metal sheet of variable radius and length, and was well suited to operation at 13.56 MHz.¹⁰ Magnetronde treatments were not, strictly speaking, MFH treatments as they are known today, as they were conducted without any implanted magnetic materials. Instead, the Magnetronde relied on deep-tissue eddy current heating alone, a mechanism of action sometimes called “inductothermy.”²⁵

A review of the literature on the Magnetronde shows that the tolerable power loadings were, as would be expected, strongly dependent on the body part being treated, and the geometry and extent of the applied field. Oleson¹¹ reported on the operating powers and efficiencies of clinical Magnetronde systems designed for the torso, thigh, and neck, indicating that the typical loadings, applied continuously in treatment sessions up to 1 h long, were ca. 750, 450, and 330 W,

TABLE I. Physical dimensions, magnetic field amplitude (measured in the central transverse plane, at a radius corresponding to the interface between the subcutaneous fat and muscle layers), and power loading characteristics of three variants of the Magnetrote electromagnetic heating system that was used clinically in the 1970s and 1980s.¹¹

Characteristic	Torso	Thigh	Neck
Magnetrote radius (cm)	24.75	11.0	11.0
Magnetrote length (cm)	28.6	7.9	1.9
Muscle/fat boundary radius (cm)	14.0	7.0	7.0
Field at muscle/fat boundary ($A\ m^{-1}$)	64	170	188
Applied power (W)	900	600	600
Loading efficiency (%)	83%	76%	55%
Loading power (W)	747	456	330

respectively (Table I). Similarly, Storm *et al.*^{8,12} referred to Magnetrote torso treatments at absorbed power levels of 500 to 1000 W. As such, the 200 W reported by Brezovich *et al.* was in fact significantly smaller than that reported by Oleson and Storm *et al.* as typical for the Magnetrote at that time.

The Magnetrote data reported by Oleson included measurements of the magnetic field amplitudes in the central transverse planes of the three systems. These data are listed in Table I for the cylinder radii r_{int} corresponding to the interface between the subcutaneous fat and the muscle layers in the torso, thigh, and neck. They allow a comparison to be made with the Brezovich criterion by considering the corresponding $P_v(r_{int})$ power densities, using Eq. (8). This requires estimates of the electrical conductivity σ of the tissue at the 13.56 MHz frequency applied by Oleson and Brezovich. For this, we use the latest data available through the ITIS database²⁶—see Table II—and we follow Oleson¹¹ and assume that the maximal power density will be associated with the muscle layer closest to the subcutaneous fat layer, on the basis that (a) the skin layer is too thin and too proximal to the thermal sink of the environment for it to be the primary site for tolerability effects to manifest, (b) the subcutaneous fat layer has a low σ and so does not experience significant heating, and (c) the muscle has the highest σ and will, therefore, experience the largest induced eddy current.

The results of these $P_v(r_{int})$ calculations are shown in Table III using the reported data from Brezovich¹⁴ and Oleson.¹¹ Also shown in Table III is another metric,

TABLE II. Electrical conductivities σ (in $S\ m^{-1}$) of selected human tissues in ≤ 1 and 13.56 MHz electromagnetic fields.²⁶ (*Datapoint estimated by assumed correlation with frequency-dependent non-directional muscle values; **datapoints estimated by averaging over the three organs.)

Tissue	σ at ≤ 1 MHz	σ at 13.56 MHz
Bone (cortical)	0.01	0.05
Muscle (non-directional)	0.46	0.63
Muscle (transverse to fibers)	0.12	0.16*
Fat (including subcutaneous)	0.08	0.06
Skin	0.15	0.24
Viscera (liver/kidney/spleen)	0.25**	0.48**

TABLE III. Local power densities $P_v(r_{int})$ and maximal specific absorption rates SAR_{max} in muscle tissue of electrical conductivity σ_{muscle} at the $r = r_{int}$ interface between muscle and subcutaneous fat in the torso, thigh, and neck, calculated using Eq. (8) and data from Tables I and II, for eddy currents induced by an axial field of amplitude H_0 and frequency $f = 13.56$ MHz.

Parameter	Torso ¹⁴	Torso ¹¹	Thigh ¹¹	Neck ¹¹
r_{int} (cm)	14.0	14.0	7.0	7.0
H_0 ($A\ m^{-1}$)	35.8	64	170	188
$H_0 f$ ($MA\ m^{-1}\ s^{-1}$)	485	870	2300	2550
σ_{muscle} ($S\ m^{-1}$)	0.63	0.63	0.16	0.16
$P_v(r_{int})$ ($mW\ cm^{-3}$)	22.7	72.5	32.5	39.7
SAR_{max} ($mW\ g^{-1}$)	20.8	66.5	29.8	36.4

$$SAR_{max} = P_v(r_{int}) / \rho_{muscle}, \tag{10}$$

which we introduce as a somewhat more intuitive means of reporting the maximal specific absorption rates (power absorbed per unit mass) at the muscle/fat interface, obtained using $\rho_{muscle} = 1.09\ g\ cm^{-3}$ as the density of muscle tissue.²⁶

On inspection of the $H_0 f$, $P_v(r_{int})$, and SAR_{max} metrics in Table III, it is notable that the thigh and neck $H_0 f$ values are ca. 3 to 5 times higher than the torso $H_0 f$ values, while for $P_v(r_{int})$ and SAR_{max} , there is no such divergence. This is logical, as the $P_v(r_{int})$ and SAR_{max} metrics intrinsically take into account the scale of the body part being treated, while the $H_0 f$ metric does not. This points to the latter being better suited than the former as indicators of clinical tolerability; indeed, metrics analogous to $P_v(r_{int})$ and SAR_{max} are reported in the literature in the context of clinical systems design. For example, the Magforce GmbH clinical MFH system used for the torso and cranium was designed assuming a value of $25\ mW\ cm^{-3}$ as the maximum allowable peripheral heating level.¹⁶

At this point, it is also interesting to follow the suggestion of Kozissnik *et al.*¹⁹ and draw a parallel between the safety considerations employed in magnetic resonance imaging (MRI) and those in MFH, given that the lower range of alternating field frequencies employed in MRI systems may be similar to those used in MFH systems. In particular, the latest IEC 60601-2-33 standard²⁷ on the safety and essential performance characteristics of MRI equipment includes a summary of recommended SAR limits for the exposure of different body regions to spatially localized radio frequency fields—see Table IV. It may be noted here that the standard presents lower SAR limits (in the range 2 to $10\ mW\ g^{-1}$) for homogeneous-field extended-treatment-volume

TABLE IV. Summary of data from the IEC 60601-2-33 standard for safety and essential performance of MRI equipment regarding allowable Local SAR levels (specific absorption rates, in $mW\ g^{-1}$, measured over any 10 g of tissue and averaged over 6 min) for the operating modes and body regions indicated. Reprinted with permission from IEC 60601-2-33ed. 4.0 (2022). Copyright 2022 IEC Geneva, Switzerland. www.iec.ch.

Operating mode	Head	Trunk	Extremities
Normal	10	10	20
First level controlled	20	20	40
Second level controlled	>20	>20	>40

systems such as whole-body scanners. However, in our opinion, the limits associated with local exposure in MRI, as given in Table IV, are more appropriate, as they better reflect the inhomogeneous field distributions that are a feature of current clinical MFH systems.⁶

It is notable in Table IV that the allowable levels of exposure depend on the operating mode. “Normal” means a mode of operation of the MR equipment in which none of the outputs has a value that can cause physiological stress to patients; “First Level Controlled” means that one or more outputs of the equipment may cause physiological stress to patients and needs to be controlled by medical supervision; and “Second Level Controlled” means that one or more outputs reach a value that can produce significant risk for patients, for which explicit ethical approval is required.²⁷

Comparing the SAR_{max} limits for MFH in Table III with the First Level Controlled Local SAR limits for MRI in Table IV, it is apparent that with one exception, they all lie between 20 and 40 $mW g^{-1}$. The exception is the $SAR_{max} = 66.5 mW g^{-1}$ for Magnetrode treatments of the torso.¹¹ It is interesting here to note a report by Storm *et al.*⁸ on the clinical side effects of such treatments, viz. profuse sweating, skin flushing, an up to 1 °C rise in core temperature, elevated pulse and respiratory rates, and increased blood pressure. It is also interesting to note that despite this catalogue of side effects, the clinical opinion expressed by Storm *et al.* is that “an absorbed power density to 1000 watts generally was well tolerated in our patients, with virtually no normal tissue injury.”⁸ This is a reminder that the question of what is “tolerable” for a potentially life-saving intervention in a clinical setting is quite different to what is tolerable in a healthy volunteer study.

Finally, it is worth noting the influence of the duty cycle on tolerability. Magnetrode treatment protocols typically involved 60 min of continuous exposure to the time-varying field. In contrast, the IEC 60601-2-33 Local SAR limits refer to an averaged exposure over 6 min, and furthermore, it is noted that shorter duration treatments may be at higher values: “the SAR limit over any 10 s period shall not exceed two times the stated values.”²⁷ This dependency is logical, given that the power deposited into any given tissue volume will disperse into the surrounding tissue and/or environment with a relaxation time constant τ that is dependent on the thermal diffusivity κ of the tissue as well as on the geometry of the system. For example, in a long cylinder of radius r , it can be shown²⁸ that $\tau \cong r^2/4\kappa$. Hence, for the torso case with muscle of diffusivity $\kappa = 1.31 cm^2 s^{-1}$,²⁶ at $r = 14.0 cm$, $\tau \cong 37 s$ is a characteristic time for the dissipation of heat away from the loading site, while for the thigh or neck at $r = 7.0 cm$, $\tau \cong 9 s$.

IV. HUMAN TOLERANCE TESTS

To further illustrate and explore the tolerability factors described earlier, we report here on two volunteer studies that were performed in our laboratory using a variety of magnetic field geometries and duty cycles. Both studies were undertaken following Institutional Research Ethics Committee review and approval.

In study 1, 330 kHz time-varying magnetic fields were applied continuously, for 5 min, to four different sites (wrist, forearm, ankle, and calf), in 13 volunteers. The field was generated using a 3-turn solenoid coil and had an amplitude $H_o(r)$ ranging from 5.73 $kA m^{-1}$ on axis (at $r = 0$) to 8.76 $kA m^{-1}$ at $r = 6.6 cm$, the largest measured limb radius. (As a benchmark reference and with limiting assumptions and caveats as discussed in the supplementary material, we note that the maximum $H_o f = 2890 MA m^{-1} s^{-1}$ used here was ca. 2.1×

corresponding, scaled, Brezovich criterion value.) Local increases in skin temperature (see Fig. 1) were monitored using a thermal imaging camera directed at the central plane of the coil.

Study 2 was run independently to study 1 and involved 15 volunteers, 12 of whom had not participated in the first study. In this study, the field was applied on a duty cycle of 67%—15 min of 2 min on, 1 min off—that is the same as is currently being used in the clinical treatment of pancreatic cancer.⁶ This study was conducted in two parts. In study 2A, a 242 kHz axial field was applied to the thigh using a 3-turn solenoid (a larger version of that used in study 1), at amplitudes ranging from 6.69 $kA m^{-1}$ on axis to 10.43 $kA m^{-1}$ at $r = 8.0 cm$, the largest measured thigh radius. The maximum $H_o f = 2525 MA m^{-1} s^{-1}$ here was ca. 2.2× the corresponding, scaled, Brezovich criterion value (see the supplementary material). In study 2B, a magnetic field generator manufactured by Resonant Circuits Limited for clinical applications⁶ containing a single-sided 2-turn coil in the shape of a curved ellipse was used to direct 330 kHz magnetic fields into the torso. The maximal field amplitude (normal to the skin surface) in this case was 4.9 $kA m^{-1}$, this being for the skin at closest approach to the coil, touching the coil housing. The observed increases in skin temperature, monitored using a thermal probe taped to the skin in the central plane of the thigh coil, or directly under the current-carrying part of the torso coil, showed a saw-tooth response that followed the on-off cycling of the field (see Fig. 2).

The $SAR_{max} = P_v(r_{int})/\rho_{muscle}$ metric was evaluated for the initial 2 min of heating for each of the study 1 and study 2A axial-field experiments, where $P_v(r_{int})$ was estimated using Eq. (6) and $\sigma = 0.12 S m^{-1}$ from Table II. [N.B.: Eq. (6) was used rather than Eq. (7) because $H_o(r)$ was not constant; however, $H_o(r)$ was well described by a third-order polynomial function of r , and the integration was straightforward.] These calculations used limb dimensions as measured for each of the participants, and it was assumed that the interface

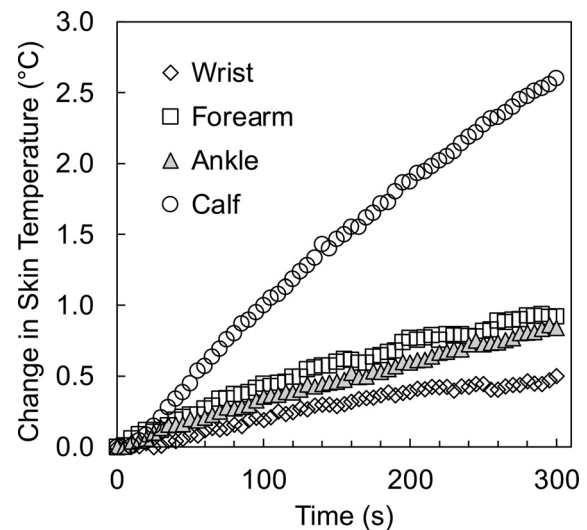


FIG. 1. Study 1 results: increases in local skin temperature at four sites (wrist, forearm, ankle, and calf), averaged across 13 individuals, due to eddy current heating from an axial magnetic field of amplitude $H_o(r)$ that ranged from 5.7 $kA m^{-1}$ (on axis, at $r = 0$) to 8.7 $kA m^{-1}$ (at $r = 6.5 cm$, the largest measured limb radius), and frequency $f = 330 kHz$, applied continuously for 5 min.

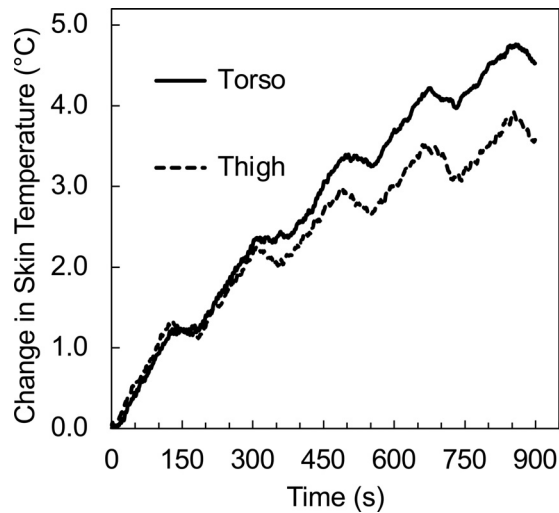


FIG. 2. Study 2 results: increases in local skin temperature, averaged across 15 individuals, due to eddy current heating applied with a 67% duty cycle (15 min of 2 min on, 1 min off). Thigh: axial field, amplitude from 6.5 kA m^{-1} on axis to 10.1 kA m^{-1} at $r = 8.0 \text{ cm}$, the largest measured thigh radius, and frequency $f = 242 \text{ kHz}$. Torso: single-sided field from a curved elliptical coil, maximal amplitude 4.9 kA m^{-1} at closest skin-coil distance, and frequency $f = 330 \text{ kHz}$.

between muscle and subcutaneous fat was at a radius $r_{\text{int}} = r_{\text{skin}} - d$, where the thickness d was taken to be 1.2 mm for the wrists and forearms, 2.8 mm for the ankles and calves, and 5.7 mm for the thighs.²⁹ These case-by-case SAR_{max} values are plotted against the observed increase in skin temperature, $\Delta T_{(t=0 \text{ to } 120 \text{ s})}$, in Fig. 3. A linear fit to the data, passing through the origin, has a Pearson coefficient $R_p = 0.89$ and a Spearman coefficient $R_s = 0.87$, both of which, being close to 1, indicate an underlying linear correlation. Such a correlation is expected only if thermal conduction and diffusion effects are

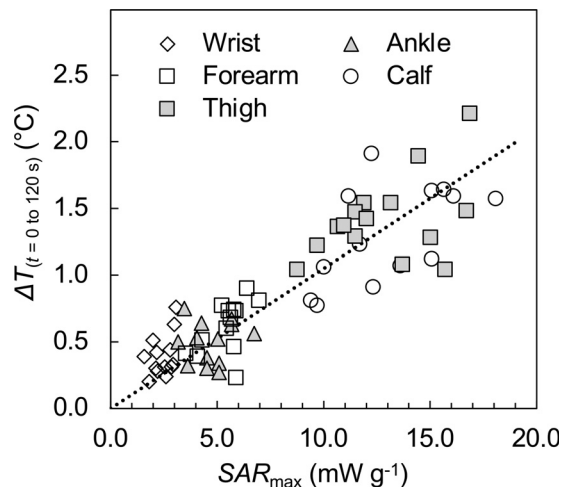


FIG. 3. Initial increase (first 2 min) in local skin temperature for each of the study 1 and study 2A experiments in which a time-varying magnetic field was applied axially, as a function of the calculated SAR_{max} metric. The dotted line is a fit to the data which indicates a linear correlation between the two metrics.

negligible,¹¹ which appears, therefore, to be the case in these initial heating experiments.

The non-axial-field coil geometry used in study 2B precludes application of the SAR_{max} metric estimation method to that data. However, a feature of the self-optimizing resonant-circuit-based magnetic field generator used in study 2 was that it was possible to estimate the loading power (the amount of power being directed into the load, i.e., the tissue), in each experiment, by monitoring the amplitude of the resonant current. This metric varies from person to person in accordance, at least in part, with the degree to which their body part ‘fills’ the magnetic coil. Figure 4 shows a plot of the observed maximum difference in skin temperature, ΔT_{max} , over the full 15 min of both the thigh and torso experiments vs the loading power. A reasonably strong linear correlation is evident for the torso data ($R_p = R_s = 0.82$), but for the thigh data, the correlation is weaker ($R_p = 0.51$, $R_s = 0.48$). Nevertheless, there appears to be a definite positive association between eddy current heating and loading powers.

The physiological aspects of the eddy current heating were further investigated in both studies by measuring each participant’s heart rate, systolic and diastolic blood pressure, and blood oxygenation levels before and after each experiment. No clear trends were observed in any of the physiological metrics, in either study. In study 2, participants were also invited to fill out a questionnaire at the conclusion of each session. When asked to rate their experience of the experiments, with regard to heat, on a scale from 1 = “not at all uncomfortable,” 2 = “not so uncomfortable,” 3 = “somewhat uncomfortable,” 4 = “very uncomfortable,” and 5 = “extremely uncomfortable,” the mean ratings from 14 respondents were 1.14 and 1.07 in studies 2A and 2B, respectively. This indicates that on the basis of both quantitative and qualitative metrics, the nonspecific heating effects associated with the experiments performed were, in all cases, very well tolerated.

V. FINITE ELEMENT ANALYSIS

Although the Brezovich $H_0 f$ parameter and the maximal specific absorption rate SAR_{max} are simple and convenient rules-of-thumb as MFH design metrics, there is no doubt that they are highly simplified model parameters that neglect many important considerations. These

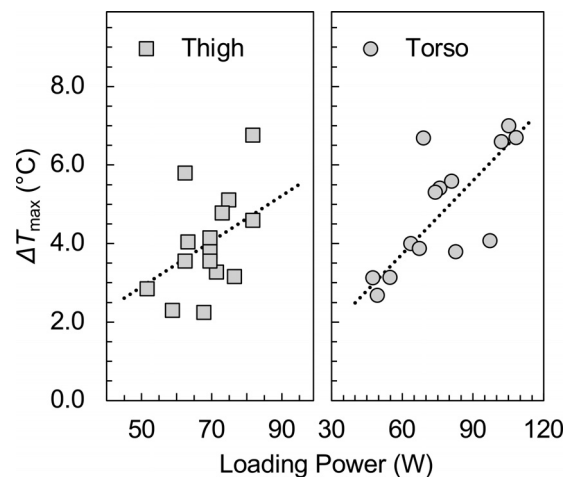


FIG. 4. Maximum observed change in local skin temperature over the full 15 min of the study 2 experiments, as a function of the amount of power delivered into the tissue. The dotted lines are straight line fits, passing through the origin.

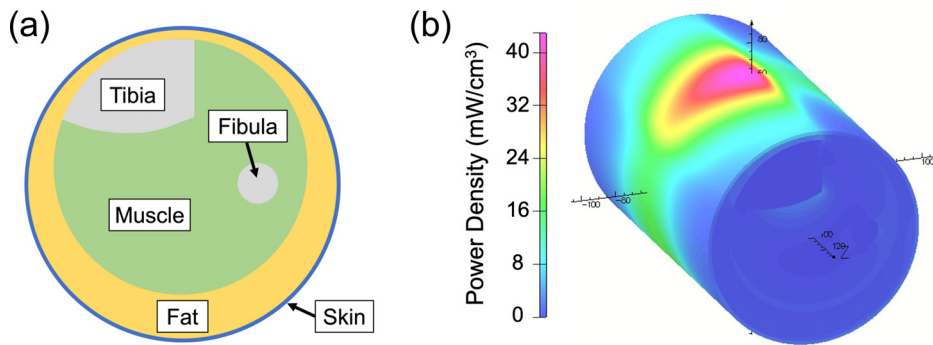


FIG. 5. (a) Simplified cross section of the human calf, showing the different tissue compartments of bone (tibia and fibula), muscle, fat, and skin. (b) Modeled eddy current induced power density at the radius of the skin, subject to an axial time-varying magnetic field as in study 1, showing a hot spot in the vicinity of the tibia.

include the effects of perfusion and metabolism on the physiological tolerability of a given thermal load, and the influence of application characteristics such as the duty cycle and environmental control. It is beyond the scope of this Perspective article to survey all such factors; however, there are two aspects of improved modeling that may be conveniently illustrated, which are relevant to the human tolerance studies described earlier, viz., anatomical “hot spots” and non-axial-field geometries.

Clinically observed MFH hot spots have been reported at skin folds and at bone surfaces⁵ and have been modeled in detail for the prospective clinical modality of magnetic particle imaging.³⁰ Here, we use the commercial Opera-3D finite element analysis package (Dassault Systèmes UK Ltd) to estimate local SAR levels in the human calf, under comparable applied field conditions to those used in study 1. The results, summarized in Fig. 5, clearly show a hot spot of increased SAR around the anterior of the calf, where the tibia lies closest to the skin. (This same feature had been noted, in passing, in the thermal camera images used to record temperatures in study 1.) As may have been expected, the calculated anterior SAR_{skin} at $r_{skin} = 6.2$ cm of ca. 40 mW g^{-1} is significantly higher than the $SAR_{max} \cong 15 \text{ mW g}^{-1}$ estimated from Eq. (6) at that radius. The calculated posterior SAR_{skin} of ca. 18 mW g^{-1} is also slightly higher than the calculated SAR_{max} ; this may be attributed to the relatively thick layer of low-electrical-conductivity subcutaneous fat in that region leading to slightly higher eddy currents and more heating there.

For the non-axial-field geometry of the study 2B torso experiments, the freely available FEMM software package was used,³¹ and the tissue of the torso was treated as a cylindrical “slab,” as shown in Fig. 6. The calculations here focused on the eddy currents induced in the tissue in closest proximity to the 2-turn coil. (Note here that only

one needs only to consider the component of the magnetic field that is normal to the skin surface, as this is the part that generates the circulating current in the tissue.) In this case, the modeled SAR_{skin} in the skin directly under the coil is ca. 29 mW g^{-1} . This level fell by 50% at radii ± 4 cm from the coil radius.

As one further consideration, it is interesting to adopt the approach to local SAR tolerability outlined in the IEC 60601-2-33 standard and to estimate what the calculated SAR_{skin} levels would be if they were measured over a minimum of 10 g of tissue and averaged over 6 min. For the Study 1 hot spot in Fig. 5, we estimate that if averaged over 10 g of skin tissue and 6 min, this is ca. 20 mW g^{-1} ; while for the study 2B hot spot with a 67% duty cycle, we estimate it is ca. 19 mW g^{-1} . Both of these are rather low levels, well in line with the First Level Controlled limits of the standard (Table IV), and a good deal lower than the clinically acceptable Magnetrotde levels (Table III). In this context, it is perhaps not surprising that the participants in the human volunteer studies experienced no notable discomfort, in any of the experiments.

Finally, we note that another option to limit the effects of surface hot spots is to employ some form of local remediation. Kumar *et al.*²⁰ describe one such approach, which involves surface cooling using a controlled-flow water jacket. As described further in the supplementary material, we have modeled another approach, which is to apply an electrically conductive material pad—one could envision a saline-impregnated cotton patch—directly over the anticipated hot spot, so as to provide a parallel path outside the body for the eddy current. In principle, the latter could be simple to implement, and as such, it might be a useful aspect of clinical application of MFH in regions of the body where hot spots are unavoidable due to anatomical features such as the proximity of bone to the skin, as was the case in Study 1.

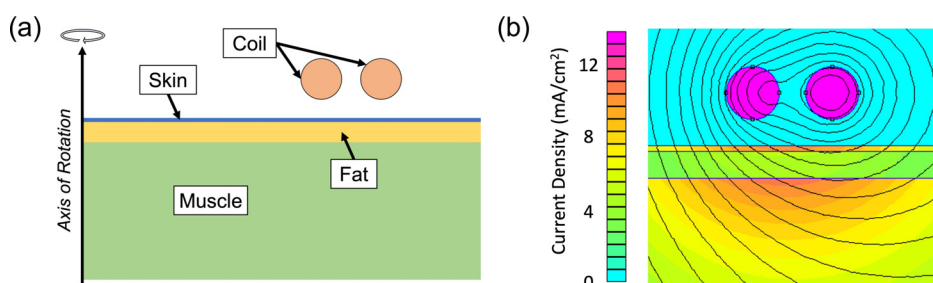


FIG. 6. (a) Simplified cross section of the human torso, showing the different tissue compartments of muscle, fat, and skin, in a region near to the 2-turn coil used in study 2B. (b) Modeled current density in the tissue slab, showing that the largest eddy currents flow in the skin directly underneath the coil.

VI. DISCUSSION AND CONCLUSIONS

Clinical safety and tolerability factors are important facets of the development of any therapeutic intervention, and this applies also to MFH magnetic field generators. However, in the MFH literature, many instances may be found where an unqualified reference is made to the Brezovich criterion as an arbiter of what is and is not acceptable, purely on the basis of whether the H_0f product happens to fall below or above $485 \text{ MA m}^{-1} \text{ s}^{-1}$. This is not the fault of the parameter itself: when used in the context and with proper appreciation for its origin and derivation (as outlined in Sec. II), it is a perfectly reasonable design parameter for some clinical MFH systems. However, that does not mean that there might not be preferable metrics that might be used, that might be less liable to misuse and misapplication, and more closely aligned with established tolerability metrics already used in other disciplines.

We propose, as an alternative to H_0f , the SAR_{max} metric, this being the maximum specific absorption rate (SAR, in W kg^{-1} or mW g^{-1}) of eddy-current-induced power absorbed per unit mass of tissue, measured over a minimum mass of 10 g of tissue and averaged in time over 6 min of normal operation of the MFH intervention. (In treatment protocols with durations of more than 6 min, the SAR_{max} should be evaluated at different timepoints throughout the treatment and the maximal value used.) The mass and time averaging here are intended to take into account both the spatial and temporal aspects of heat transport in the body and are aligned to the protocols established for tolerance testing of MRI equipment operating with local transmit coils in the IEC 60601-2-33 standard.²⁷

The SAR concept is already well known and frequently used in clinical settings and has the advantage of being likely to be readily understood and accepted. The SAR_{max} metric also has the advantage of being relatively easily estimated, either from first-principles calculations (as illustrated in Secs. III and IV) or from finite element analysis simulations (as in Sec. V), and may also be directly measured in suitable phantoms.¹¹ Furthermore, as shown in Sec. IV, it looks to be a reliable metric when compared to human volunteer data, and it is adaptable to the consideration of hot spots and the treatment of non-axial-field geometries, as featured in Sec. V.

It may be noted that another possible alternative to the H_0f metric is the “loading power,” which we have used here to describe the engineering-based parameter, wherein the manufacturers of MFH systems can monitor the total amount of power deposited into the subject. This corresponds to the method described in IEC 60601-2-33 for whole-body or partial-body MRI scanners using volume transmit coils. We consider this to be a useful option in some cases, especially where the mass of tissue being exposed to the MFH field is known, so that an effective SAR, averaged over the entire mass, may be defined. However, we think that in most cases, the SAR_{max} metric is likely to be more informative.

Turning to the question of what should be taken as safe limits for SAR_{max} for clinical applications of MFH, once again it seems that valuable lessons may be learned from the clinical MRI experience. We recommend that as a starting point for a given application, the limits presented in Table IV should be considered, e.g., that for a First Level Controlled MFH indication where it is intended that the operation of the MFH generator would be under medical supervision but not requiring any particular patient-specific ethical approval, then SAR_{max} should not exceed 20 mW g^{-1} in the torso or head, and 40 mW g^{-1} in the limbs, these values being averaged over 10 g of tissue and 6 min of

normal treatment. It should be noted that this statement does not preclude the use of higher SAR_{max} levels should the clinical benefit justify it; indeed, a glance at the SAR_{max} values listed in Table III that were used clinically for many years of the Magnetrote treatment shows that in many cases, elevated SAR_{max} levels may, indeed, be justified. However, as a rule-of-thumb, the levels presented in Table IV would look to be a good starting point.

Finally, it is perhaps useful to remark on the application of clinical tolerability limits in preclinical settings. On the basis of the assumption that the electrical conductivity of non-human mammalian tissue is comparable to human tissue of the same type, it seems logical that the SAR associated with MFH-generated eddy current heating in animal tissue should be treated as if it were human tissue. Indeed, it is interesting to apply the SAR_{max} approach to data reported on nonspecific heating in mice:³² doing so shows that no adverse effects were observed in the animals at levels up to 24 mW g^{-1} (at $H_0 = 5.6 \text{ kA m}^{-1}$ and $f = 153 \text{ kHz}$, assuming $r_{\text{mouse}} = 20 \text{ mm}$ and $\sigma_{\text{muscle}} = 0.46 \text{ S m}^{-1}$), but that at 44 mW g^{-1} ($H_0 = 7.6 \text{ kA m}^{-1}$), morbidity and injuries were observed. Reducing the duty cycle from 100% to 50%, and thereby lowering the SAR to 22 mW g^{-1} , it returned the MFH to tolerable levels for the animals.³² As such, it appears that the SAR_{max} metric can, indeed, be usefully applied to animal studies of MFH.

To conclude, it is clear that the SAR_{max} tolerability metric is grounded in fundamental science, that it is well defined and clinically recognizable, that it may be estimated via both experimental and *in silico* routes, and that it can be used in both clinical and preclinical settings. Furthermore, we propose that there is a ready parallel to be made between the established guidelines for local SAR limits for MRI, and guidelines for SAR_{max} limits for MFH. As such, it is our hope that the future adoption and use of the SAR_{max} tolerability metric may prove to be a useful step toward the development of standards and methods for testing the safety and tolerability of magnetic field hyperthermia equipment.

SUPPLEMENTARY MATERIAL

See the supplementary material for further details on the volunteer studies and on the thermal modeling studies.

ACKNOWLEDGMENTS

The authors thank the International Electrotechnical Commission (IEC) for permission to reproduce Information from its International Standards. All such extracts are copyright of IEC, Geneva, Switzerland. All rights reserved. Further information on the IEC is available from www.iec.ch. IEC has no responsibility for the placement and context in which the extracts and contents are reproduced by the author, nor is IEC in any way responsible for the other content or accuracy therein.

AUTHOR DECLARATIONS

Conflict of Interest

The authors have no conflicts to disclose.

Author Contributions

Martin Kwok: Investigation (equal). **Cliona Maley:** Investigation (equal). **Asher Dworkin:** Investigation (equal). **Simon Hattersley:**

Formal analysis (equal); Supervision (equal); Writing – review & editing (equal). **Paul Southern:** Formal analysis (equal); Supervision (equal); Writing – review & editing (equal). **Quentin Pankhurst:** Conceptualization (lead); Formal analysis (equal); Writing – original draft (lead).

DATA AVAILABILITY

The data that support the findings of this study are available within the article and its supplementary material.

REFERENCES

- ¹D. Ortega and Q. A. Pankhurst, “Magnetic hyperthermia,” in *Nanoscience: Nanostructures through Chemistry*, edited by P. O’Brien (RSC Publishing, 2012), Vol. 1, pp. 60–88.
- ²Q. A. Pankhurst, J. Connolly, S. K. Jones, and J. Dobson, “Applications of magnetic nanoparticles in biomedicine,” *J. Phys. D* **36**, R167–R181 (2003).
- ³Q. A. Pankhurst, N. K. T. Thanh, S. K. Jones, and J. Dobson, “Progress in applications of magnetic nanoparticles in biomedicine,” *J. Phys. D* **42**, 224001 (2009).
- ⁴R. R. Baker, C. Payne, Y. Yu, M. Mohseni, J. J. Connell, F. Lin, I. F. Harrison, P. Southern, U. S. Rudrapatna, D. J. Stuckey, T. L. Kalber, B. Siow, L. Thorne, S. Punwani, D. K. Jones, M. Emberton, Q. A. Pankhurst, and M. F. Lythgoe, “Image-guided magnetic thermoseed navigation and tumor ablation using a magnetic resonance imaging system,” *Adv. Sci.* **9**, 2105333 (2022).
- ⁵B. Thiesen and A. Jordan, “Clinical applications of magnetic nanoparticles for hyperthermia,” *Int. J. Hyperthermia* **24**, 467–474 (2008).
- ⁶See <https://tinyurl.com/3zfkurth> for “Vall d’Hebron enrolls the first patient in a clinical trial designed to treat locally advanced pancreatic cancer with nanoparticles” (Vall d’Hebron Institute of Oncology, 2023).
- ⁷Activity indicated by ca. 14 000 hits in the Web of Science database at <https://tinyurl.com/yphx7rmj> for the keyword “magnetic hyperthermia,” and ca. 900 publications per annum for the last 5 years (2023).
- ⁸F. K. Storm, W. H. Harrison, R. S. Elliott, and D. L. Morton, “Normal tissue and solid tumor effects of hyperthermia in animal models and clinical trials,” *Cancer Res.* **39**, 2245–2251 (1979).
- ⁹F. K. Storm, W. H. Harrison, R. S. Elliott, and D. L. Morton, “Hyperthermic therapy for human neoplasms: Thermal death time,” *Cancer* **46**, 1849–1854 (1980).
- ¹⁰R. S. Elliott, W. H. Harrison, and F. K. Storm, “Hyperthermia: Electromagnetic heating of deep-seated tumors,” *IEEE Trans. Biomed. Eng.* **BME-29**, 61–64 (1982).
- ¹¹J. R. Oleson, “Hyperthermia by magnetic induction. 1. Physical characteristics of the technique,” *Int. J. Radiat. Oncol. Biol. Phys.* **8**, 1747–1756 (1982).
- ¹²F. K. Storm, R. S. Elliott, W. H. Harrison, and D. L. Morton, “Clinical RF hyperthermia by magnetic-loop induction: A new approach to human cancer therapy,” *IEEE Trans. Microwave Theory Tech.* **30**, 1149–1157 (1982).
- ¹³W. J. Atkinson, I. A. Brezovich, and D. P. Chakraborty, “Usable frequencies in hyperthermia with thermal seeds,” *IEEE Trans. Biomed. Eng.* **BME-31**, 70–75 (1984).
- ¹⁴I. A. Brezovich, “Low frequency hyperthermia: Capacitive and ferromagnetic thermoseed methods,” in *Medical Physics Monograph No. 16: Biological Physical and Clinical Aspects of Hyperthermia*, edited by B. R. Paliwal, F. W. Hetzel, and M. W. Dewhirst (American Institute of Physics, 1988), pp. 82–110.
- ¹⁵Evidenced by ca. 340 papers citing Atkinson 1984 and ca. 145 citing Brezovich 1988 being listed in the Web of Science database at <https://tinyurl.com/yphx7rmj> (2023).
- ¹⁶A. Jordan, P. Wust, H. Fahling, W. John, A. Hinz, and R. Felix, “Inductive heating of ferrimagnetic particles and magnetic fluids—Physical evaluation of their potential for hyperthermia,” *Int. J. Hyperthermia* **9**, 51–68 (1993).
- ¹⁷R. Hergt and S. Dutz, “Magnetic particle hyperthermia—biophysical limitations of a visionary tumour therapy,” *J. Magn. Magn. Mater.* **311**, 187–192 (2007).
- ¹⁸G. Bellizzi and O. M. Bucci, “On the optimal choice of the exposure conditions and the nanoparticle features in magnetic nanoparticle hyperthermia,” *Int. J. Hyperthermia* **26**, 389–403 (2010).
- ¹⁹B. Kozissnik, A. C. Bohorquez, J. Dobson, and C. Rinaldi, “Magnetic fluid hyperthermia: Advances, challenges, and opportunity,” *Int. J. Hyperthermia* **29**, 706–714 (2013).
- ²⁰A. Kumar, A. Attaluri, R. Mallipudi, C. Cornejo, D. Bordelon, M. Armour, K. Morua, T. L. Dewese, and R. Ivkov, “Method to reduce non-specific tissue heating of small animals in solenoid coils,” *Int. J. Hyperthermia* **29**, 106–120 (2013).
- ²¹B. E. Kashevsky, S. B. Kashevsky, V. S. Korenkov, Y. P. Istomin, T. I. Terpinskaya, and V. S. Ulashchik, “Magnetic hyperthermia with hard-magnetic nanoparticles,” *J. Magn. Magn. Mater.* **380**, 335–340 (2015).
- ²²G. Bellizzi, O. M. Bucci, and G. Chirico, “Numerical assessment of a criterion for the optimal choice of the operative conditions in magnetic nanoparticle hyperthermia on a realistic model of the human head,” *Int. J. Hyperthermia* **32**, 688–703 (2016).
- ²³A. R. Tsiapla, A. A. Kalimeri, N. Maniotis, E. Myrovali, T. Samaras, M. Angelakeris, and O. Kalogirou, “Mitigation of magnetic particle hyperthermia side effects by magnetic field controls,” *Int. J. Hyperthermia* **38**, 511–522 (2021).
- ²⁴B. Herrero de la Parte, I. Rodrigo, J. Gutiérrez-Basoa, S. Iturrizaga Correcher, C. Mar Medina, J. J. Echevarría-Uraga, J. A. García, F. Plazaola, and I. García-Alonso, “Proposal of new safety limits for in vivo experiments of magnetic hyperthermia antitumor therapy,” *Cancers* **14**, 3084 (2022).
- ²⁵J. H. Young, M. T. Wang, and I. A. Brezovich, “Frequency/depth-penetration considerations in hyperthermia by magnetically induced currents,” *Electron. Lett.* **16**, 790–791 (1980).
- ²⁶P. A. Hasgall, F. Di Gennaro, C. Baumgartner, E. Neufeld, B. Lloyd, M. C. Gosselin, D. Payne, A. Klingeböck, and N. Kuster, see <https://www.itis.swiss/database/> for “ITIS Database for thermal and electromagnetic parameters of biological tissues, Version 4.1” (2022).
- ²⁷See <https://tinyurl.com/b99au7z2> for “IEC 60601-2-33:2022—Medical electrical equipment—Part 2-33: Particular requirements for the basic safety and essential performance of magnetic resonance equipment for medical diagnosis” (International Electrotechnical Commission, 2022).
- ²⁸A. L. McKenzie, “Physics of thermal processes in laser-tissue interaction,” *Phys. Med. Biol.* **35**, 1175–1209 (1990).
- ²⁹P. Storchle, W. Muller, M. Sengeis, S. Lackner, S. Holasek, and A. Furrhapter-Rieger, “Measurement of mean subcutaneous fat thickness: Eight standardised ultrasound sites compared to 216 randomly selected sites,” *Sci. Rep.* **8**, 16268 (2018).
- ³⁰O. Dössel and J. Bohnert, “Safety considerations for magnetic fields of 10 mT to 100 mT amplitude in the frequency range of 10 kHz to 100 kHz for magnetic particle imaging,” *Biomed. Tech.* **58**, 611–621 (2013).
- ³¹D. C. Meeker, see <https://www.femm.info/> for “Finite Element Method Analysis, Version 4.2” (2018).
- ³²R. Ivkov, S. J. DeNardo, W. Daum, A. R. Foreman, R. C. Goldstein, V. S. Nemkov, and G. L. DeNardo, “Application of high amplitude alternating magnetic fields for heat induction of nanoparticles localized in cancer,” *Clin. Cancer Res.* **11**, 7093s–7103s (2005).